China Ocean Eng., Vol. 30, No. 4, pp. 521– 534

DOI 10.1007/s13344-016-0032-8 ISSN 0890-5487

Dynamic Analysis of Turret-Moored FPSO System in Freak Wave*

TANG You-gang (唐友刚)[a, b, 1], LI Yan (李　焱)[a, b], WANG Bin (王　宾)[a, b],
LIU Shu-xiao (刘树晓)[a, b] and ZHU Long-huan (朱龙欢)[a, b]

[a] *School of Civil Engineering*, *Tianjin University*, *Tianjin 300072*, *China*
[b] *State Key Laboratory of Hydraulic Engineering Simulation and Safety*, *Tianjin University*, *Tianjin 300072*, *China*

(Received 30 January 2015; received revised form 31 March 2015; accepted 12 June 2015)

ABSTRACT

Freak wave is the common wave which has significant wave height and irregular wave shape, and it is easy to damage offshore structure extremely. The FPSOs (Floating Production Storage and Offloading) suffer from the environment loads, including the freak wave. The freak waves were generated based on the improved phase modulation model, and the coupling model of FPSO-SPM (Single Point Mooring) was established by considering internal-turret FPSO and its mooring system. The dynamic response characteristics of both FPSO and SPM affected by the freak wave were analyzed in the time domain. According to the results, the freak waves generated by original phase modulation model mainly affect the 2nd-order wave loads. However, the freak waves which are generated by random frequencies phase modulation model affect both 1st-order and 2nd-order wave loads on FPSO. What is more, compared with the irregular waves, the dynamic responses of mooring system are larger in the freak waves, but its amplitude lags behind the peak of the freak wave.

Key words: *turret-moored FPSO*; *freak wave*; *phase modulation*; *internal turret*; *couple dynamic analysis*

1. Introduction

The freak wave, also known as rouge wave or anomalous wave, is a common type of wave in the ocean. With its huge wave height and irregular shape, scientists can hardly draw a general law or prediction for the freak wave. Because of its extreme wave amplitude, vessels and offshore structures are easily damaged or lost under this severe wave condition. The freak waves often appear in the area where the navigation is well-developed or oil and gas are rich. As a permanent moored structure in the production area, both FPSO and its mooring system suffer from various environment loads, including the potential risk of freak wave's load.

Numerous work on observation of freak waves has been completed in both ocean and laboratory, such as Touboul *et al*. (2006), Li et al. (2009), Yan and Ma (2010) and Cui *et al.* (2012, 2013). What is more, in recent decades, various works have been done in the field of freak wave's generation and prediction. El-Bedwehy (2014) investigated the nonlinear freak wave in electron–hole quantum GaAs semiconductor plasma via a nonlinear Schrödinger equation (NLS). Dyachenko *et al.* (2012, 2014)

* This work was financially supported by the National Natural Science Foundation of China (Grant Nos. 51279130 and 51479134).
1 Corresponding author. E-mail: tangyougang_td@163.com

applied canonical transformation to Zakharov water wave equation to simplify drastically fourth-order terms in Hamiltonian, proving this equation being suitable for the simulation of sea surface wave including freak waves appearing. Different mathematical methods for generating such wave have been developed (Slunyaev, 2006; Zakharov *et al.*, 2006; Hu *et al.*, 2014; Hu and Zhang, 2014), and the efficiency was compared (Zhao *et al.*, 2009). Also lots of studies on FPSO system's dynamic response have been done, such as Gui *et al.* (2014) and Zhao *et al.* (2013). However, less attention has been paid to freak effect on the dynamic response of the offshore structures. Rudman and Cleary (2013) used SPH (Smoothed Particle Hydrodynamic) to simulate the fully non-linear dynamics of a large breaking wave on a TLP (Tension Leg Platform) and predicted the maximum tension on each tendon. Zhao *et al.* (2014) used an improved model governed by the Navier–Stokes equation to simulate the freak wave impact on a floating body in the numerical basin, also compared with a designed physical experiment. Deng *et al.* (2014) investigated the impact of freak wave sequence on the motion behavior of a semisubmersible in the time domain, and they considered that the maximum motion responses depend not only on the largest wave crest amplitude but also on the time lags between successive giant waves. Gu *et al.* (2013) generated freak waves through improved phase modulation model, and the motion characteristics were analyzed for a TLP. Xiao *et al.* (2009) calculated a TLP's hydrodynamic coefficients through three-dimensional potential theory, and also carried out the TLP's dynamic analysis in the freak wave.

The objective of this work is to study the motion of turret-moored FPSO and dynamic characteristics of SPM in freak wave. Firstly, based on the Longuet-Higgins wave model, the wave spectrum was dispersed in various frequencies, and then the freak wave elevation was generated according to modulating the phases which was corresponding to the chosen frequencies. Secondly, the hydrodynamic coefficients of an FPSO was calculated in the frequency domain based on the three-dimensional potential theory, also the motion equation was established in the time domain according to the couple dynamic analysis, and the dynamic response results of FPSO and SPM were shown in the time domain. In addition, the influence of different freak wave generation methods on SPM's dynamic responses were also studied.

2. Generation Method of Freak Wave

For the simulation of the freak wave, the linear method and the nonlinear method can be used. At present, the linear method is widely used to generate freak wave, the linear superposition method based on the Longuet-Higgins model is simple and rapid, and the waveform is stable. So the freak wave is generated by the linear method in this paper.

2.1 Longuet-Higgins Wave Model

Assuming that the stochastic wave propagating along the positive x-axis is decomposed into the sum of a number of regular wave units.

$$\eta(t)=\sum_{n=1}^{N} a_n \cos\left(k_n x-\omega_n t+\varepsilon_n\right), \tag{1}$$

where N is the number of wave components. For each regular wave component, a_n denotes the wave amplitude, ω_n is the circular frequency, k_n is the wave number, and ε_n is the random phase angle. Wave amplitude a_n can be expressed by wave energy spectrum,

$$\sum_{\omega_n}^{\omega_n+\Delta\omega_n} \frac{1}{2} a_n^2 = S_\eta(\omega_n)\Delta\omega_n , \tag{2}$$

where $\Delta\omega_n$ is the frequency interval between two adjacent wave frequencies, and $S_\eta(\ )$ is the wave spectrum function. This is a typical method to simulate random waves in the laboratory.

2.2 Numerical Simulation of Freak Waves

Different from random waves, the freak waves are formed by wave energy concentration at a point. The approaches used to generate random waves are not applicable for freak wave simulation because of the low efficiency. Some special numerical methods are adopted in freak wave simulation, including the phase modulation method, random wave superposed with transient wave, etc (Liu and Zhang, 2010). In the present study, the freak waves were simulated by using the phase modulation model.

2.2.1 *Definition of Freak Wave*

Klinting and Sand (1987) first proposed the definition of freak wave, holding that the following three conditions should be met for the shape of freak waves:

(1) The ratio of the freak wave height to the significant wave height should not be smaller than 2, i.e. $H_{\max}/H_s \geq 2$.

(2) The ratio of the wave crest height to the freak wave height should not be smaller than 0.65, i.e. $\eta_c/H_{\max} \geq 0.65$.

(3) The ratio of the freak wave height to the adjacent wave height should not be smaller than 2, i.e. $H_{\max}/H_1 \geq 2$ and $H_{\max}/H_2 \geq 2$.

In the present study, the three conditions mentioned above were used in order to compare the efficiency of different freak wave simulation methods. Freak waves were generated based on JONSWAP spectrum. Wave parameters were selected according to the FPSO's design survival wave condition: the significant wave height H_s=12.7 m, peak period T_p=14.9 s, peakedness parameter γ =3.0 and the number of regular wave components N=1000.

2.2.2 *Phase Modulation Model*

The phase modulation model was proposed by Longuet-Higgins, and the wave spectrum was uniformly divided into M parts in the wave frequency range. After choosing some components to adjust their initial phases and summing up all of the wave components, the freak wave was generated. There are a majority of methods to modulate the initial phase. Among such methods, the improved phase modulation model has an extra high simulation efficiency, so the method is selected to simulate freak wave. The method is as follows.

It is assumed that the freak wave occurs at the position x_c and time t_c, and the number of wave

components M equals M_1+M_2, and then the equation of the wave surface elevation can be transferred into the following form:

$$\eta(t)=\sum_{n=1}^{M_1+M_2} a_n \cos\left(k_n x-\omega_n t+\varepsilon_n\right). \tag{3}$$

As a large-scale wave is expected at the given position and time in the resultant wave consisted of the latter M_2 wave components, ε_n in the latter part of Eq. (3) was adjusted to make the wave elevation at position x_c and time t_c, in order to simulate the freak wave. With this method, the generated freak wave's elevation is shown in Fig. 1.

However, according to the study, it is shown that the simulated freak wave generated by this equal frequency spacing is pseudo random, and the extreme crest will repeat with a period of $2\pi/\Delta\omega$, which means that it does not match the actual situation of wave. So the random frequency spacing has been used to solve this problem. Besides, if some specified wave frequency components are chosen to generate freak wave, the energy distribution of the freak wave will not be homogeneous. In order to remove this influence, a method of random frequency components selection was used to simulate freak wave. In this method, the frequencies used in the second part of the equation's right side are chosen randomly. A freak wave elevation produced by this random frequency phase modulation method is shown in Fig. 2.

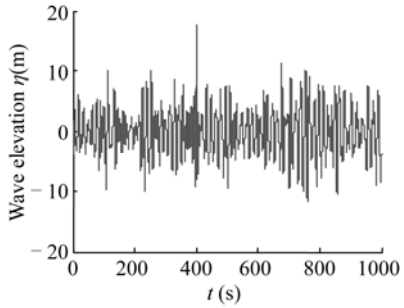

Fig. 1. Freak wave elevation generated by original method.

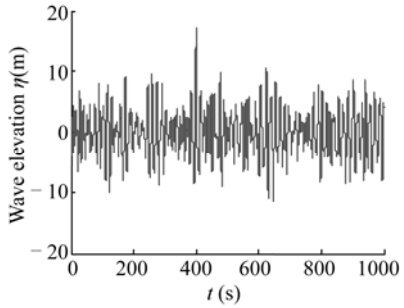

Fig. 2. Freak wave elevation generated by random method.

By using these two methods, 1000 freak wave elevations were generated respectively. For each freak wave, the simulation time was 1000 s, with time step of 0.1 s. And the extreme crest was focused at the position $x=0$ and time $t=400$ s. According to the determination conditions mentioned in Section 2.2.1, the statistical results of different freak wave generation methods' quality comparison are shown in Table 1.

Table 1 Comparison of freak waves generated by different phase modulation model

Method	H_{max}/H_s			η_c/H_{max}			H_{max}/H_1	H_{max}/H_1
	Min.	Max.	Number*	Min.	Max.	Number*	Number*	Number*
Original	1.40	3.46	746	0.19	0.77	176	646	418
Random	1.33	4.13	944	0.53	0.79	288	764	481

*Number means the number of freak waves that meet the corresponding determination condition.

According to Table 1, it can be easily inferred that both the random frequency component phase

modulation method and the original phase modulation method have very high efficiency in generation of freak waves, but the random method has higher precision. What is more, among the 1000 elevations generated by the random method, there are 32 time series satisfying the strong non-linear condition that $\eta_c / H_s > 0.7$ (Gu *et al.*, 2013). Therefore, it shows that rational freak wave can be generated by such random method.

3. Motion Equations of the FPSO-SPM Coupled System

An internal turret-moored FPSO system typically consists of two parts: one part is the large body structure like the ship hull; the other is composed of slender structures such as mooring lines and risers. These two parts are coupled. There are two available methods to evaluate the response of the system, according to the modelling approach of mooring and riser systems. One method is the quasi-static analysis, which is often used at an initial planning stage. The other is the dynamic analysis, and the couple dynamic analysis is often used in the time domain.

3.1 Motion Equation of the FPSO

The FPSO's motion is determined by the system's inertia, damping, restoring stiffness, and the environmental conditions. The mooring system provides restoring stiffness for the FPSO and the FPSO's motion has an impact on the mooring system's motion in turn. So FPSO and the mooring system are coupled each other. The motion equation of the FPSO in the time domain can be written as:

$$\begin{aligned}&\left[m_{ji}+A_{ji}(\infty)\right]\ddot{x}_i(t)+\int_0^t r_{ji}\left(t-\tau\right)\dot{x}_i(t)\mathrm{d}\tau+D_{ji}\dot{x}_i(t)+c_{ji}x(t)\\&\quad=F_{wa\,j}^{(1)}(t)+F_{wa\,j}^{(2)}(t)+F_{wi\,j}(t)+F_{cu\,j}(t)+F_{mor\,j}(t),\end{aligned}\tag{4}$$

where, m_{ji} is the mass matrix element; $A_{ji}\left(\infty\right)$ is the added mass matrix element when the frequency is infinity; $r_{ji}\left(t-\tau\right)$ is the retardation function matrix element; D_{ji} is the linear damping matrix element; c_{ji} is the restoring stiffness matrix element; $F_{\mathrm{wa}\,j}^{(1)}(t)$, $F_{\mathrm{wa}\,j}^{(2)}(t)$, $F_{\mathrm{wi}\,j}(t)$, $F_{\mathrm{cu}\,j}(t)$, and $F_{\mathrm{mor}\,j}(t)$ are the first-order wave load, second-order wave load, wind load, current load, and mooring load, respectively. Two approaches are available to calculate the second-order wave load: the Newman Approximation and the full QTF (Quadratic Transfer Function) method.

3.2 Motion Equation of the SPM System

In dynamic analysis, the mooring lines are discretized into finite elements, for each of which the dynamic equilibrium equation can be written as:

$$R_{\mathrm{I}}\left(r,\ddot{r},t\right)+R_{\mathrm{D}}\left(r,\dot{r},t\right)+R_{\mathrm{S}}\left(r,t\right)=R_{\mathrm{E}}\left(r,\dot{r},t\right),\tag{5}$$

where, the three terms on the left side of the equation are the inertia force, damping force, and internal structural reaction force, respectively; while the one on the right side denotes the external force. r, $\dot{r}$, and $\ddot{r}$ are the FPSO's displacement, velocity, and acceleration, respectively. The external force on the mooring line accounts for weight and buoyancy of the line, forced displacements due to FPSO

motions and wave loads on the line, drag and wave acceleration terms in Morison equation, and specified discrete nodal point forces.

3.3 Computational Model

A 100000-tonne internal turret-moored FPSO serving in the South China Sea is modelled. The water depth is 90 m and the main parameters of the FPSO are listed in Table 2.

Table 2 Main parameters of an FPSO in the South China Sea

Parameters	Value
Length over all (m)	232.5
Length between perpendiculars (m)	225.0
Breadth moulded (m)	46.0
Depth moulded (m)	24.1
Draft (m)	15.6
Displacement (tonne)	150772
Natural period of heave (s)	11.1
Natural period of roll (s)	12.6
Natural period of pitch (s)	9.9

Layout of the FPSO's mooring system and numbering of mooring lines are shown in Fig. 3. The FPSO is moored by means of three groups of lines, each with three mooring lines, which is further connected to the FPSO by the submerged turret buoy of STP (Submerged Turret Production) system. Separation of the lines within each line group is 5°, providing 110° opening between the line groups. The length of each mooring line is 894 m, and the horizontal distance from turret to anchor is 873.9 m. Each mooring line is composed of chain and wire segments as listed in Table 3.

Table 3 Characteristics of mooring line segments

Section	Length (m)	Material	Nominal diameter (mm)	Unit mass (kg/m)	Unit submerged weight (kN/m)	Breaking strength (kN)	Axial stiffness (kN)
LCS	20	Chain	147	436.5	3.723	19100	1270200
CE1	1	Connecting element			25.00		
LWS	520	Wire	150	87.2	0.661	17000	1550000
CE2	1	Connecting element			25.00		
UCS1	76.5	Chain	147	436.5	3.732	19100	1270200
UCS2	21.2	Chain	147	436.5	3.732	19100	1270200
UCS3	38.8	Chain	147	436.5	3.732	19100	1270200
UCS4	21.2	Chain	147	436.5	3.732	19100	1270200
UCS5	42.3	Chain	147	436.5	3.732	19100	1270200
CE3	1	Connecting element			25.00		
UWS	150	Wire	150	87.2	0.661	17000	1550000
CE4	1	Connecting element			25.00		

The LCS segment is attached to seabed and the UWS segment is attached to the turret. The UCS2, UCS3, and UCS4 segments are distributed with 17 clump weights and each clump weight is 68.7 kN. Since the dynamic analysis method is used, the hydrodynamic coefficients of mooring line are

determined according to the BV and DNV standards. Details of the coefficients are shown in Table 4, where C_{dx} and C_{dy} are mean longitudinal and transverse drag coefficients, and C_{ax} and C_{ay} represent the longitudinal and transverse added mass coefficients, respectively.

Table 4 Hydrodynamic coefficients of mooring line

	C_{dx}	C_{dy}	C_{ax}	C_{ay}	Diameter
Chain	1.15	2.4	0.5	1	132 mm
Wire	0	1.2	0	1	130 mm

Coordinate system and environmental condition directions are defined in Fig. 4. The turret of the FPSO system is defined at the origin of the coordinate system. Since the single point mooring system is designed for permanent mooring of the FPSO for the 100-year typhoon condition, 100-year return period environmental condition is selected when performing time domain analysis. The freak wave generated with the aforementioned method is selected as the wave condition. NPD spectrum is selected as the input wind spectrum and the average wind velocity is 38.8 m/s. The current is treated as a steady flow and the surface current velocity is 2.24 m/s. In consideration of the weather vane effect of single point mooring FPSO system, wind, wave and current are defined as the same direction in order to evaluate the influence of freak wave. Study on the restoring characteristics of the mooring system has shown that the stiffness is least when the environment load is along the direction between two groups of lines. The environment loads direction is selected as 210° based on the practical ocean situation.

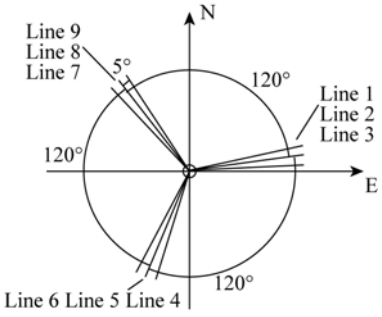

Fig. 3. Layout of mooring system.

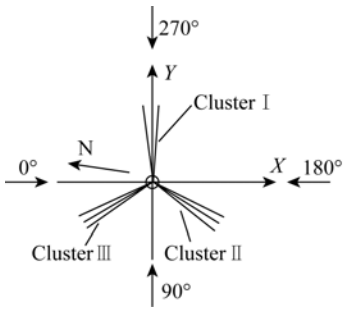

Fig. 4. Coordinate system and definition of environment loads direction.

4. FPSO's Dynamic Characteristics in Freak Wave

FPSO and the mooring system are modelled in the SESAM program module DeepC. The coupled analysis model is shown in Fig. 5.

In order to compare the impact behavior of freak wave on the dynamic characteristics of mooring system, the freak waves generated according to Section 2 are the input into DeepC before the couple dynamic analysis. Since the freak wave is a transient process, a 3-hour duration of time domain simulation is not needed. The actual length of simulation is 1000 s, with the time step of 0.1 s. H_{max}/H_s and η_c/H_{max} are abbreviated as a_1 and a_2 hereinafter.

Fig. 5. FPSO-SPM coupled analysis model.

4.1 Freak Wave Generated by the Ordinary Phase Modulation Method

A freak wave elevation time series generated by the ordinary phase modulation method is shown in Fig. 6. For short, we name it as Freak Wave 1. In Freak Wave 1, parameter a_1 is 2.251, and a_2 is 0.727, as a strong non-linear freak wave mentioned above. Fig. 7 shows FPSO's heave and pitch motion. In the time history, we cannot observe the obvious increasing motion at the given time t = 400 s. Furthermore, FPSO's motion at this time is less than the motion under the random wave at time t = 650 s. Since the heave and pitch motions belong to high frequency motion, such motions are mainly affected by the 1st-order wave load. As Fig. 8 shows, the 1st-order wave load of this FPSO does not increase at the given time t = 400 s, and this is the very reason why the FPSO's high-frequency motion was not affected by the freak wave. However, in the time history of the 2nd-order wave load of the FPSO, which is also an important component of environment load, there appears a significant peak since the time when the freak wave crest occurs. Fig. 9 presents this status, and we can preliminarily draw a conclusion that the freak wave generated by the original phase modulation method chiefly impacts the 2nd-order wave load which is the major component to influence the FPSO's low-frequency motion in the horizontal plane. Thus, the mooring system's dynamic response is affected indirectly, as shown in Fig. 10. Both the turret's horizontal motion and the mooring lines' tension increase significantly, but both peaks lag behind the crest of the freak wave. According to this change, we can expect that the ordinary phase modulation method will amplify the freak wave's effect on the 2nd-order wave load.

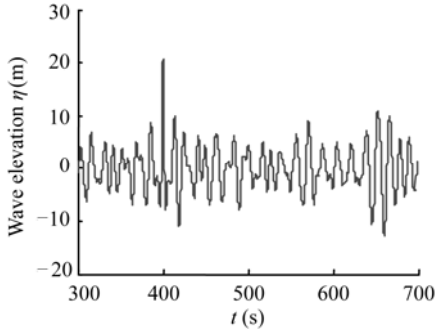

Fig. 6. Elevation of Freak Wave 1.

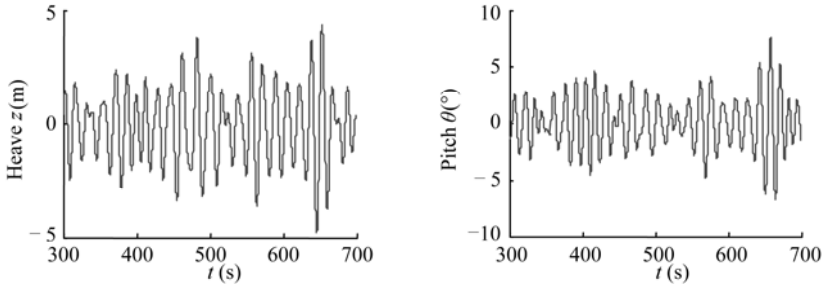

Fig. 7. FPSO's heave and pitch motion in Freak Wave 1.

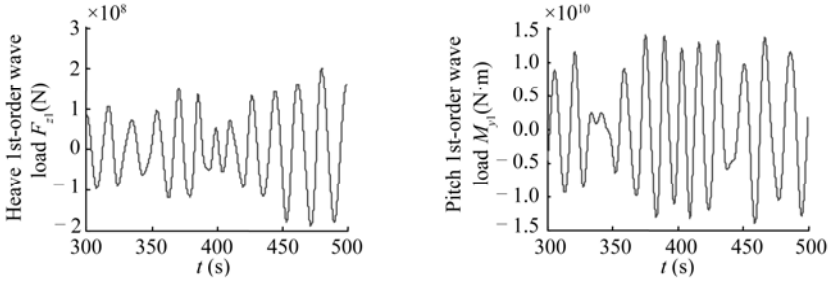

Fig. 8. FPSO's heave and pitch 1st-order wave loads in Freak Wave 1.

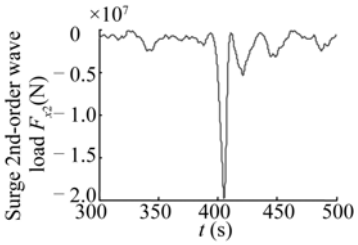

Fig. 9. FPSO's surge 2nd-order wave load in Freak Wave 1.

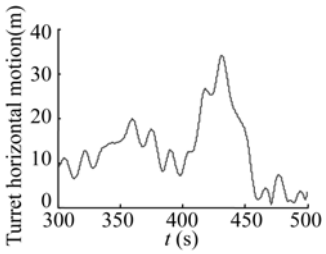

Fig. 10. Turret's motion in Freak Wave 1.

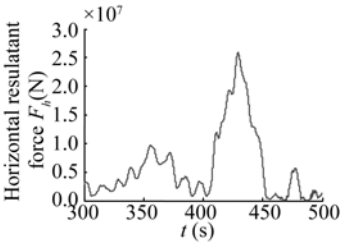

Fig. 11. Horizontal resultant force of all lines' tension in Freak Wave 1.

In order to verify the conclusion that the ordinary method will affect the 2nd-order wave load heavily, the number of freak wave's components was added to produce a bigger freak crest, as shown in Fig. 12. Also for short, we call it Freak Wave 2, and its parameters a_1 and a_2 are 5.888 and 0.657, respectively. In this wave, FPSO's 1st-order and 2nd-order wave load are displayed in Figs. 13 and 14. From these figures, we can significantly find the freak crest's influence on FPSO's wave loads. That is to say, with the increasing freak wave's components, the increased 1st-order wave load can be observed. However, the incensement is still less significant than that of the 2nd-order load, as the statistic results show in Table 5. In addition, the freak crests appear more than once, and the crests between pre and post the given time t = 400 s are strongly freak, too. Owing to such wave peaks, four amplitude peaks are observed in the 1st-order wave load, but only once in the 2nd-order wave load. As a consequence, the wave elevations generated by the original method fit the determinant conditions of the freak wave, but the influence on the 2nd-order wave load is much larger than that on

the 1st-order wave load.

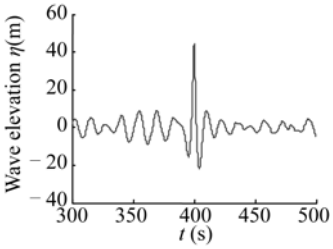

Fig. 12. Elevation of Freak Wave 2.

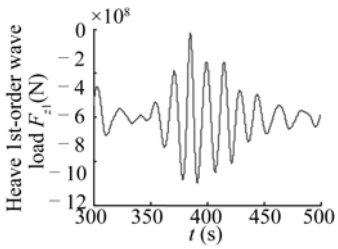

Fig. 13. FPSO's heave 1st-order wave load in Freak Wave 2

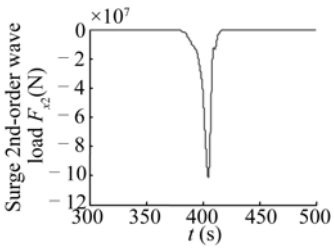

Fig. 14. FPSO's surge 2nd-order wave load in Freak Wave 2.

Table 5 Comparison of the calculated wave load's amplitude

	Wave height of crest	Amplitude of the 1st-order wave load	Amplitude of the 2nd-order wave load
Freak Wave 1	28.59 m	1.35×10^8 N	1.98×10^7 N
Freak Wave 2	74.78 m	3.81×10^8 N	1.01×10^8 N
Ratio	2.616	2.829	5.090

4.2 Freak Wave Generated by the Random Frequency Components Selection Phase Modulation Method

In order to modify the defects caused by the original method, the method selecting some frequency components to generate the freak waves was used. Then by using these wave elevations as input, the dynamic responses of the FPSO-SPM coupling system were calculated. A wave elevation (Freak Wave 3) which is similar to the time series of Fig. 6 is displayed in Fig. 15, and a comparative analysis is carried out. Wave's parameters a_1 and a_2 are 2.207 and 0.714, respectively. The heave and pitch motions in Freak Wave 3 are shown in Fig. 16, and we can easily find that the motions at given time t = 400 s increase obviously. With the random frequency selection method, the wave energy of the freak crest will not distribute in a specified range, and both low and high frequency wave loads will reflect the effect of the freak peak, as shown in Figs. 17 and 18. Owing to the incensement of the 2nd-order wave load shown in Fig. 18, the mooring system's dynamic responses, such as turret's motion (Fig. 19) and resultant force (Fig. 20), meet a large peak which is almost 1.5 times the previous peak. However, the amplitude of the response lags behind the crest of the freak wave.

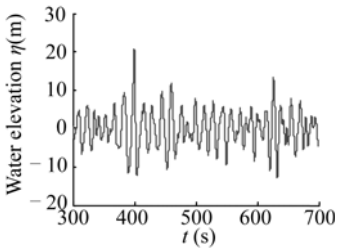

Fig. 15. Elevation of Freak Wave 3.

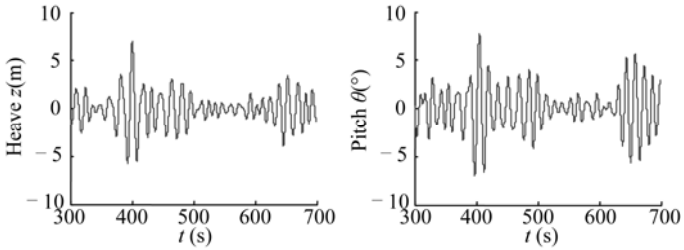

Fig. 16. FPSO's heave and pitch motions in Freak Wave 3.

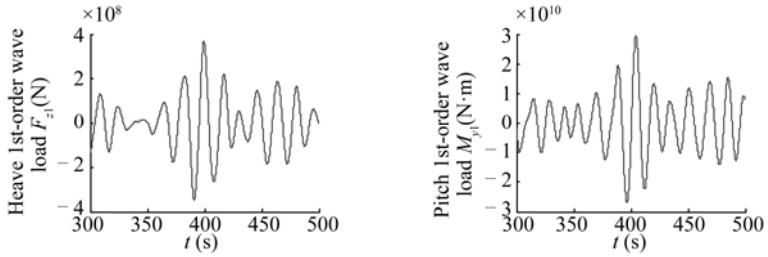

Fig. 17. FPSO's heave and pitch 1st-order wave loads in Freak Wave 3.

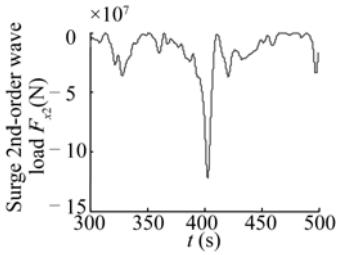

Fig. 18. FPSO's surge 2nd-order wave load in Freak Wave 3.

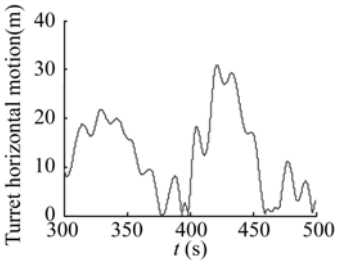

Fig. 19. Turret's motion in Freak Wave 3.

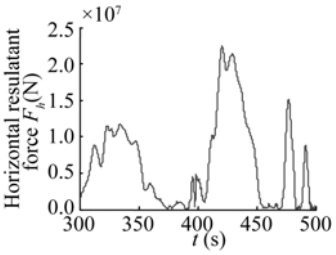

Fig. 20. Horizontal resultant force of all lines' tension in Freak Wave 3.

4.3 Dynamic Responses of the FPSO System in Freak Wave

Owing to the burst characteristics of the freak wave, the loads on FPSO and its mooring system can be considered as an impact load. When an impact load acts on the system, the dynamic response amplitude may appear in the forced or free vibration process (Tang, 2002). The relative magnitudes of natural frequency and pulse frequency are the keys to determine the dynamic response in which process the peak appears. The natural frequencies of FPSO pitch and heave motions are close to the wave frequency, so the extreme motions are captured at the exact time when the freak peak appears. However, as shown in Fig. 23, the SPM response's natural frequency is much lower than the wave frequency, so the peaks of turret's motion and horizontal resultant mooring force will lag behind the crest of the freak wave, and this is demonstrated by the time series as shown in Figs. 19 and 20.

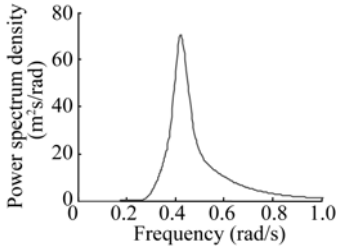

Fig. 21. Wave spectrum.

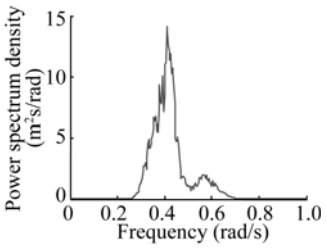

Fig. 22. Power spectrum density for heave motion.

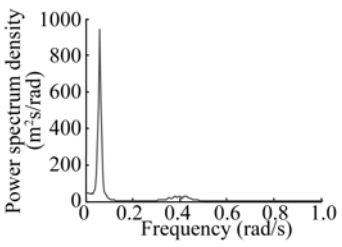

Fig. 23. Power spectrum density for turret's motion.

For further studying the freak wave's influence on the SPM system, a comparison analysis about the mooring system's dynamic response between Freak Wave 3 and irregular wave is presented, and the results are shown in Table 6. We can draw a conclusion from the results that, under the freak wave

conditions, the mooring system's dynamic responses increase obviously, including the mooring lines tension and turret's horizontal motion. Compared with the normal irregular wave condition, the maximal line tension, the maximal horizontal resultant force of all lines' tension and the maximal turret horizontal displacement increase by 48.5%, 57.5% and 26.7%, respectively.

Table 6 Comparison of freak wave's and random wave's influence on SPM

	Maximum line tension (N)	Maximum horizontal resultant force (N)	Maximum turret horizontal offset (m)
Freak wave	9.00×10^6	2.24×10^7	30.984
Irregular wave	6.06×10^6	1.42×10^7	24.451

5. Conclusions

The improved phase modulation methods are used to simulate freak waves, and the dynamic responses of a turret-moored FPSO are analyzed under different freak wave's time series. The main conclusions are drawn as follows.

(1) Both the originally improved phase modulation method and random frequency components selection phase modulation method have high efficiency on simulating the freak waves, and the random method has higher efficiency than the original method.

(2) The 2nd-order wave load on FPSO is overestimated under the original method's freak wave. Only by greatly increasing the modulated components, the freak crest's influence on the 1st-order wave loads will appear, but the freak wave does not accord with the fact. With the random method, both the 1st-order and 2nd-order loads reflect the freak wave's amplification effect on the dynamic response, and this will directly lead to the increase of the FPSO' motion, as well as the SPM's responses.

(3) Because of the burst characteristics, freak wave's load on the system is a kind of impact load. As the wave frequency is close to the high motions' natural frequencies, such as pitch and heave, the amplitudes of these motions appear at the exact time as the huge crest shows. However, the natural frequencies of SPM's dynamic responses are much lower than the wave frequency, so the peaks of these responses lag behind the peak of the wave elevation and appear at the free vibration process. Furthermore, compared with the irregular wave, the dynamic response of SPM increases obviously in freak waves.

(4) In this paper, different modulation methods have been used to generate freak waves, and the main purpose is to explore the dynamic responses of FPSO in freak waves. The modulation method belongs to the linear method, and it can be widely used in engineering circles. What is more, the nonlinear method is another way to generate freak waves in the numerical wave basin. Based on this method, the freak waves show nonlinear features to some extent. However, it is hard to summarize a feasible nonlinear process of the freak wave generation in the engineering field. In order to understand the difference between the linear and nonlinear methods, further studies are needed to investigate the nonlinear modelling process and dynamic analysis.

References

Cui, C., Zhang, N. C., Pei. Y. G. and Liu, Q. L., 2012. Numerical study on generation and evolution of freak waves, *Journal of Ship Mechanics*, **16**(12): 1373–1384. (in Chinese)

Cui, C., Zhang, N. C., Zuo, S. H. and Fang, Z., 2013. A study on kinematics characteristics of freak wave, *China Ocean Eng.*, **27**(3): 391–402.

Deng, Y. F., Yang, J. M. and Xiao, L. F., 2014. Influence of wave group characteristics on the motion of a semisubmersible in freak waves, *Proceedings of the 33rd International Conference on Ocean*, *Offshore and Arctic Engineering* (*ASME 2014*), San Francisco, California, USA, pp. V01AT01A045–V01AT01A045.

Dyachenko, A. I., Kachulin, D. I. and Zakharov, V. E., 2014. Freak waves at the surface of deep water, *Journal of Physics*: *Conference Series*, **510**(1): Article id. 012050.

Dyachenko, A. I. and Zakharov, V. E., 2012. A dynamic equation for water waves in one horizontal dimension, *Eur. J. Mech. B-Fluid.*, **32**, 17–21.

El-Bedwehy, N. A., 2014. Freak waves in GaAs semiconductor, *Physica B: Condensed Matter*, **442**, 114–117.

Gu, J. Y., Lv, H. N. and Yang, J. M., 2013. Dynamic response study of four column TLP in freak waves, *The Ocean Engineering*, **31**(5): 25–36. (in Chinese)

Gui, L., Tang, Y. G., Qin, Y., Yang, H. S. and Li, Y., 2014. Mooring analysis of FPSO position limiting operation in shallow water, *The Ocean Engineering*, **32**(3): 28–35. (in Chinese)

Hu, Z. Q., Tang, W. Y. and Xue, H. X., 2014. A probability-based superposition model of freak wave simulation, *Appl. Ocean Res.*, **47**, 284–290.

Hu, J. P. and Zhang, Y. Q., 2014. Analysis of energy characteristics in the process of freak wave generation, *China Ocean Eng.*, **28**(2): 193–205.

Klinting, P. and Sand, S. E., 1987. Analysis of prototype freak waves, *ASCE Special Conference Nearshore Hydrodynamics*, OH, USA, 618–632.

Li, J., Chen, G. and Yang, J. M., 2009. Simulation of deep water freak wave in laboratory, *China Offshore Platform*, (3): 22–25. (in Chinese)

Liu, Z. C. and Zhang, C. N., 2010. Numerical methods for simulating freak waves based on the Longuet-Higgins wave model theory, *Journal of Waterway and Harbor*, **31**(4): 236–241. (in Chinese)

Rudman, M. and Cleary, P. W., 2013. Rogue wave impact on a tension leg platform: The effect of wave incidence angle and mooring line tension, *Ocean Eng.*, **61**, 123–138.

Slunyaev, A., 2006. Nonlinear analysis and simulations of measured freak wave time series, *Eur. J. Mech. B-Fluid.*, **25**(5): 621–635.

Tang, Y. G., 2002. *Advanced Structural Dynamics*, Tianjin University Press, Tianjin, 24–25. (in Chinese)

Touboul, J., Giovanangeli, J. P., Kharif, C. and Pelinovsky, E., 2006. Freak waves under the action of wind: Experiments and simulations, *Eur. J. Mech. B-Fluid.*, **25**(5): 662–676.

Xiao, X., Teng, B., Gou, Y. and Ning, D. Z., 2009. Transient response of TLP under freak waves, *Port and Waterway Engineering*, (5): 9–14. (in Chinese)

Yan, S. and Ma, Q. W., 2011. Improved model for air pressure due to wind on 2D freak waves in finite depth, *Eur. J. Mech.B-Fluid.*, **30**(1): 1–11.

Zakharov, V. E., Dyachenko, A. I. and Prokofiev, A. O., 2006. Freak waves as nonlinear stage of Stokes wave modulation instability, *Eur. J. Mech. B-Fluid.*, **25**(5): 677–692.

Zhao, X. Z., Ye, Z. T., Fu, Y. N. and Cao, F. F., 2014. A CIP-based numerical simulation of freak wave impact on a floating body, *Ocean Eng.*, **87**, 50–63.

Zhao, X. Z., Sun, Z. C. and Liang, S. X., 2009. Efficient focusing models for generation of freak waves, *China*

Ocean Eng., **23**(3): 429–440.

Zhao, Z. J., Tang, Y. G., Wu, Z. R. and Li, Y., 2013. Design and research on the amplitude-frequency characteristics of a new concept multi-cylindrical FPSO, *Ship Engineering*, **35**(1): 95–98. (in Chinese)